Carcinogenesis vol.34 no.10 pp.2415–2423, 2013
doi:10.1093/carcin/bgt191
Advance Access publication June 1, 2013

Suppression of colon carcinogenesis by targeting Notch signaling

Shingo Miyamoto, Masako Nakanishi and Daniel W. Rosenberg*

Center for Molecular Medicine, University of Connecticut Health Center, 263 Farmington Avenue, Farmington, CT 06030-3103, USA

*To whom correspondence should be addressed. Tel: +1 860 679 8704; Fax: +1 860 679 7639;
Email: rosenberg@uchc.edu

Recent studies have shown that aberrant Notch signaling contributes to the pathogenesis of colorectal cancer (CRC). However, the potential therapeutic benefits of Notch pathway inhibitors, including gamma-secretase inhibitors (GSIs) on colon carcinogenesis are still unclear. In this study, the effects of the GSI, *N*-[*N*-3,5-difluorophenacetyl]-L-alanyl-*S*-phenylglycine methyl ester (DAPM) on colon carcinogenesis were investigated. *In vitro*, DAPM suppressed cell proliferation and induced the expression of Krüppel-like factor 4 (KLF4) and p21 in human colon cancer cells. Interestingly, p21-null HCT 116 cells were largely resistant to the suppressive effects of DAPM on cell proliferation compared with the parental cells. To investigate the effects of DAPM *in vivo*, colonoscopy was performed to establish the presence of colon tumors 9 weeks after azoxymethane treatment. After tumors were identified, mice were injected intraperitoneally every other day with either DAPM or vehicle for 4 weeks. The frequency of both large (>4 mm) and small (<1 mm) colon tumors was significantly reduced by DAPM treatment. Colon tumors in the DAPM-treated mice displayed increased levels of KLF4 and p21, accompanied by reduced Ki-67 staining compared with controls. Notably, in human colon tumor biopsies, KLF4 and p21 expressions were present within hyperplastic polyps, but the levels of both proteins were markedly reduced in tubular adenomas. Our results suggest that inhibition of Notch signaling by DAPM provides a potential chemopreventive strategy for patients with tubular adenomas, in part via activation of the KLF4-p21 axis.

Introduction

Despite extensive efforts to develop more effective anticancer agents, colorectal cancer (CRC) remains the second leading cause of cancer-related deaths in USA. This is due in part to the limitations of chemotherapy resulting from drug resistance and organ system toxicities. To overcome these inherent limitations associated with chemotherapy, the development of novel therapeutic strategies that can target critical cancer-related pathways is necessary.

Notch signaling is a key developmental signaling pathway that plays an important role in the determination of cell fate. In recent years, the vital role of Notch signaling in regulating a balance between proliferation, differentiation and apoptosis has been described (1,2). In mammals, four Notch genes are expressed, each of which encodes a single-pass transmembrane receptor (Notch 1–4). The interaction between Notch receptors and their ligands (Jagged 1 and 2 and Delta-like 1, 3 and 4) results in proteolytic cleavage of Notch by a γ-secretase, which releases the Notch intracellular domain (NICD) from the plasma membrane, initiating a subsequent nuclear translocation. Following nuclear translocation, NICD binds to and forms a complex with one of three transcriptional regulators, including CSL [collectively referring to C-promoter binding factor (CBF)-1, Suppressor of Hairless in Drosophila, and Lag-1 in *Caenorhabditis elegans* also known as recombination signal-binding protein Jκ (RBP-Jκ)], mastermind (MAML)-1 and p300/CBP, followed by transcriptional activation of a set of target genes, including the hairy-enhancer-of-split (*Hes*) gene family (3,4). Since Hes-1 is a transcriptional repressor, Notch signaling negatively regulates Krüppel-like factor 4 (KLF4) through its activation of Hes-1 expression (5). KLF4 is highly expressed in terminally differentiated epithelial cells in the colon (6) and is also believed to be a tumor suppressor via its ability to induce p21 expression (7).

The first report to establish an association between aberrant Notch signaling and tumorigenesis came from studies of T-cell acute lymphoblastic leukemia (8), in which a chromosomal translocation associated with ~10% of T-cell acute lymphoblastic leukemia was shown to give rise to a truncated Notch 1 protein lacking most of the extracellular domain. Following this initial observation, it was then revealed that aberrant Notch signaling was also present within solid tumors, including breast cancer, medulloblastoma, non-small cell lung carcinoma, melanoma and also CRC (9). In human CRC, inappropriate activation of Notch signaling can occur as early as the adenoma stage, but Notch activity is typically reduced as the disease progresses (10). Fre *et al.* (11) reported that transgenic expression of NICD leads to expansion of enterocytic progenitor cells, possibly contributing to the increased number of adenomas in $Apc^{Min/+}$ mice (12), a model for intestinal tumorigenesis (13,14). In addition, inactivation of Notch signaling by deletion of the Notch ligand, Jagged 1, was found to inhibit tumor growth in $Apc^{Min/+}$ mice (15). Importantly, recent reports show that treatment of mice with gamma-secretase inhibitors (GSIs), a class of drug that blocks the Notch cleavage (16), suppresses intestinal tumor formation through induction of goblet cell differentiation in adenomas in $Apc^{Min/+}$ mice (5,17).

Collectively, these findings suggest that pharmacologic inactivation of Notch signaling with the use of GSIs may have therapeutic potential in the treatment of intestinal tumors. However, these preclinical studies have mainly focused on tumor suppression in the small intestine, the primary site for tumorigenesis in the $Apc^{Min/+}$ model. Thus, the potential chemopreventive or therapeutic effects of GSI on colon carcinogenesis have not been established. Therefore, in the following study, we evaluated the effects of the GSI, *N*-[*N*-3,5-difluorophenacetyl]-L-alanyl-*S*-phenylglycine methyl ester (DAPM), in carcinogen-exposed strain A (A/J) mice (18–21), in which the location of tumors was verified by colonoscopy (22) prior to the start of drug therapy. Our findings were further extended to a panel of human colon tumors.

Abbreviations: ACF, aberrant crypt foci; AOM, azoxymethane; APC, adenomatous polyposis coli; CRC, colorectal cancer; DAPI, 4′,6-diamidino-2-phenylindole; DAPM, *N*-[*N*-3,5-difluorophenacetyl]-l-alanyl-*S*-phenylglycine methyl ester; DAPT, *N*-[*N*-3,5-difluorophenacetyl]-l-alanyl-S-phenylglycine t-butyl ester; GSI, gamma-secretase inhibitors; *Hes*, hairy-enhancer-of-split gene; i.p., intraperitoneally; KLF4, Krüppel-like factor 4; NICD, Notch intracellular domain; PBS, phosphate-buffered saline; WT, wild-type.

Materials and methods

Chemicals

Azoxymethane (AOM), a genotoxic, organotropic colon carcinogen, was purchased from Sigma Chemical Co. (St Louis, MO). Dulbecco's modified Eagle medium and fetal bovine serum were purchased from Gibco BRL (Grand Island, NY). Antibodies directed against Notch 1 (#3608), cleaved Notch (#4147), KLF4 (#4038) and horseradish peroxidase-conjugated anti-rabbit antibody (#7074), were obtained from Cell Signaling Technology (Beverly, MA). Antibody for detecting p21 was purchased from BD Pharmingen (San Diego, CA). Antibody for detecting KLF4 by immunofluorescence was purchased from Santa Cruz Biotechnology (Santa Cruz, CA).

Cell culture

HCT116 and SW480 cells were maintained in Dulbecco's modified Eagle medium supplemented with 10% (vol/vol) fetal bovine serum and 1% penicillin/streptomycin. The wild-type (WT) HCT116 cells and the $p21^{-/-}$ variant cells were generously provided by Dr Bert Vogelstein (Johns Hopkins University,

Baltimore, MD) and maintained in McCoy's 5A medium supplemented with 10% (vol/vol) fetal bovine serum and 1% penicillin/streptomycin. All cell lines were maintained at 37°C in a humidified 5% CO_2 atmosphere.

Cell proliferation

All cell lines were seeded into 24 well plates under the growth conditions described above. Twenty-four hours after seeding, the cells were treated with DAPM (0–100 μM) for the various times indicated in the figure legends (0–72 h) and cell proliferation was assessed using the 3-(4,5-dimethylthiazole-2-yl)-2,5-diphenyl tetrazolium bromide assay.

Western blotting

Following treatment with DAPM, colon cancer cells were washed twice with phosphate-buffered saline (PBS) and lysed in buffer containing 50 mM Tris, pH 8.0, 0.1% sodium dodecyl sulfate, 1.0% IGEPAL CA-630, 0.5% sodium deoxycholate and 150 mM NaCl supplemented with protease and phosphatase inhibitors. Following centrifugation at 14 000 r.p.m. for 5 min, the supernatant was removed and quantified for total protein. Denatured proteins (40 μg) were separated using sodium dodecyl sulfate–polyacrylamide gel electrophoresis on a 10% polyacrylamide gel and transferred onto Immobilon-P membranes (Millipore, Billerica, MA). After blocking with dry milk for 1 h, the membranes were incubated with the appropriate specific primary antibody (Supplementary Table 1, available at *Carcinogenesis* Online), followed by the corresponding horseradish peroxidase-conjugated secondary antibody (1:10 000). The blots were developed using enhanced chemiluminescence western blotting detection reagents. The intensity of each band was analyzed using Image J.

Mice

Five-week-old male A/J mice were purchased from The Jackson Laboratories (Bar Harbor, ME). Mice were maintained in a temperature-controlled, light-cycled room and allowed free access to drinking water and standard diet (LM-485, Harlan Teklad). Animals were weighed and checked every other day for signs of weight loss or lethargy indicating intestinal obstruction or anemia associated with tumors. Animal experiments were conducted upon approval from the Center for Laboratory Animal Care Committee (CLACC), The University of Connecticut Health Center. All mice were quarantined for 1 week prior to experimentation.

Animal treatment

A total of 30 male A/J mice were divided into the control and experimental groups. The experimental protocol is shown in Supplementary Figure S1, available at *Carcinogenesis* Online. Mice were injected with 10 mg/kg AOM or saline intraperitoneally (i.p.) once a week for 6 weeks. DAPM solubilized in dimethyl sulfoxide was suspended in PBS containing 0.5% (wt/vol) methylcellulose (Sigma). Mice were treated with 1 mg/kg body weight DAPM or vehicle control by i.p. injection every other day for a total of 4 weeks, beginning 10 weeks after the last AOM injection. One week prior to the start of DAPM treatment (week 15), mice were subjected to colonoscopic imaging to verify the presence of colon tumors. Mouse colonoscopy was performed using a modified Olympus human choledochoscope, consisting of an Olympus Exera CV-160 camera system with an Olympus CHF B160 camera unit, as described previously (22), with an insertion diameter of 3 mm. To perform the colonoscopy, mice were anesthetized by i.p. injection of Ketamine/Xylazine solution consisted of 0.6 ml ketamine (100 mg/ml), 0.4 ml xylazine (20 mg/ml) and 4 ml saline and was injected in a volume of ~8 μl per gram body weight, as described earlier (23). To clear intestinal contents, colons were flushed with sterile Hanks' balanced salt solution using an 18 g gavage needle inserted to a depth of 4 cm. The tip of the endoscope was inserted slowly into the colon to a maximum depth of 4 cm. Mice were killed at week 20 (14 weeks after the last injection of AOM) and the frequency of aberrant crypt foci (ACF) and tumors was determined. The colons were flushed with PBS, excised, measured in length (from the ileocecal junction to the anal verge), slit open longitudinally along the main axis and washed again with PBS. The colons were macroscopically inspected, and whole colons were processed for paraffin embedding, after being cut and fixed in 10% buffered formalin for at least 24 h.

Tissue sample preparation, Alcian blue staining and immunohistochemistry

The paraffin-embedded colon samples were sectioned at 7 μm thickness. Sections were deparaffinized in xylene, and Alcian blue staining was carried out as described previously with a minor modification (5). Briefly, Alcian blue was applied to the sections for 30 min at room temperature followed by counterstaining for nuclei with hematoxylin for 10 min. Thirty colon crypts were randomly selected from five mice per group, and Alcian blue-positive cells were counted. Immunohistochemistry for Ki-67 was performed as reported previously (24). The frequency of Ki-67-positive cells was determined in a total of 15 tumors harvested from 5 mice per group and counted in a high-power (×400) field.

Immunofluorescence

Following antigen retrieval, sections were blocked and incubated overnight at 4°C with anti-KLF4 and β-catenin antibodies in 2% bovine serum albumin in Tris-buffered saline. Sections were washed in Tris-buffered saline and then incubated with secondary antibodies (goat anti-mouse IgG Alexa 488 and goat anti-rabbit IgG Alexa 568; 1:200 in 2% bovine serum albumin in Tris-buffered saline; Molecular Probes) for 30 min at room temperature in the dark. Nuclei were counterstained with 4′,6-diamidino-2-phenylindole (DAPI: 1:10 000). Staining was visualized using an Olympus IX50 fluorescence microscope (Olympus Corp.).

Human subjects

Human samples were obtained from 18 patients undergoing routine screening colonoscopy at the John Dempsey Hospital (JDH) at the University of Connecticut Health Center as a part of 'A Pilot Study of Genomic Instability in Premalignant Colorectal Polyps Using High Resolution Single Nucleotide polymorphism (SNP) Arrays' study in accordance with institutional policies. In total, there were 22 samples, comprised 9 hyperplastic polyps, 12 tubular adenomas and 4 adjacent normal tissues. This study was undertaken after approval by the University of Connecticut Health Center Institutional Review Board, and all subjects provided a written informed consent.

Statistical analysis

Where applicable, data were analyzed using a Student's *t*-test (two-sided), with a $P < 0.05$ considered statistically significant.

Results

Suppression of Notch signaling activity reduces cell proliferation and increases KLF4 and p21 expression in colon cancer cell lines

Initially, the effects of GSI treatment on cell proliferation were investigated in human colon cancer cell lines. As shown in Figure 1, human HCT116 and SW480 cells were treated with 0–100 μM DAPM for 72 h. Drug treatment significantly reduced cell proliferation in both cell lines in a dose-dependent manner (Figure 1A). However, SW480 cells were less susceptible to the growth suppressive effects of DAPM compared with HCT116. Recently, Ghaleb *et al*. (5) indicated that KLF4 is a downstream repression target of Notch signaling and a potential mediator of the suppressive effects of GSI on cell proliferation. To explain the observed differential sensitivity of these two cell lines to DAPM treatment, we examined the expression of NICD, KLF4 and p21, the latter protein that is also a transcriptional target of KLF4, in the presence of increasing concentrations of DAPM (Figure 1B). In both cell lines, DAPM treatment resulted in an equivalent dose-dependent inhibition of NICD formation. Drug treatment also produced a marked increase in the levels of KLF4 and p21 in HCT116 cells. The effect on p21, however, was significantly ($P = 0.03$) attenuated in the SW480 cells (Figure 1B; Supplementary Figure S2A, available at *Carcinogenesis* Online). This latter observation may account in part for the relative resistance of SW480 cells to DAPM treatment.

p21-null colon cancer cells are resistant to cell growth inhibition induced by DAPM

Based on these results, we hypothesized that p21 plays an important role in the growth suppressive effects of DAPM. To test this possibility, we examined the effects of DAPM treatment on cell proliferation in HCT116 WT and $p21^{-/-}$ cells. As shown in Figure 1C; Supplementary Figure S2B, available at *Carcinogenesis* Online, at 48 h, 30 μM DAPM significantly ($P < 0.03$) suppressed Notch cleavage and induced the expression of KLF4 to a comparable extent in both cell lines when tested at 48 h after treatment. p21 expression was also induced by DAPM treatment in HCT116 WT cells, an effect that was associated with a significant and dose-dependent suppression of cell proliferation (Figure 1D). Importantly, $p21^{-/-}$ cells exhibited relative resistance to the suppressive effects of DAPM on cell proliferation compared with the HCT116 WT cells (Figure 1D). These results show that p21 is an important mediator for the suppression of cell proliferation resulting from inhibition of Notch signaling.

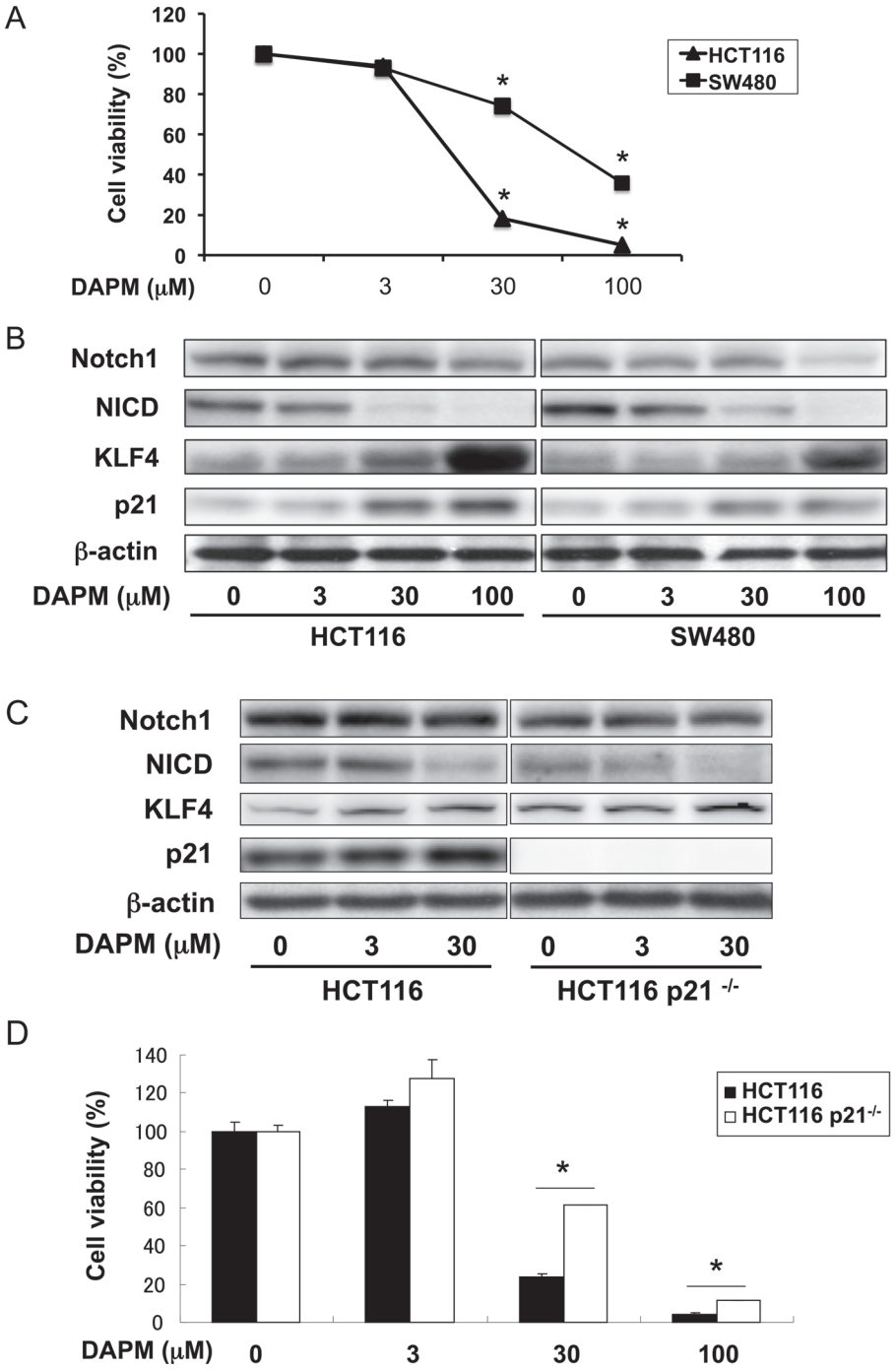

Fig. 1. Suppressive effects of DAPM on cell proliferation and Notch signaling in colon cancer cell lines. Human colon cancer cell lines HCT116 (Wt and $p21^{-/-}$) and SW480 were treated with the indicated concentration of DAPM, for either 48 or 72 h. (**A**) HCT116 and SW480 cell lines were treated with increasing concentrations of DAPM for 72 h. Cell viability was assessed using the 3-(4,5-dimethylthiazole-2-yl)-2,5-diphenyl tetrazolium bromide assay. Each data point represent the mean value of triplicate samples. *$P < 0.05$ compared with dimethyl sulfoxide treatment (Student's *t*-test). (**B**) Western blot analysis for the indicated proteins after 48 h of treatment of DAPM. The blots were reprobed using β-actin as a loading control. (**C**) HCT116 parental and $p21^{-/-}$ cell lines were treated with increasing concentrations of DAPM for 48 h. The effects of DAPM on the Notch signaling pathway were evaluated by western blot analysis for the indicated proteins after 48 h of treatment with DAPM. The blots were reprobed using β-actin as a loading control. (**D**) Both cell lines were treated with increasing concentration of DAPM for 72 h. Cell viability was assessed by 3-(4,5-dimethylthiazole-2-yl)-2,5-diphenyl tetrazolium bromide assay. Columns, mean of triplicate samples; bars, standard deviation. *$P < 0.05$ compared with HCT116 parental cells (Student's *t*-test).

GSI treatment suppresses colon carcinogenesis

Based on our *in vitro* results, we sought to determine whether GSI might elicit a protective effect against colon carcinogenesis *in vivo*. Initially, to evaluate the involvement of Notch activation in colon carcinogenesis, we examined NICD expression in AOM-induced mouse colon tumor samples. Consistent with previous reports, expression of NICD was localized to the bottom half of adjacent normal crypts (Figure 2A). Furthermore, NICD expression levels were markedly elevated throughout the epithelial compartment of AOM-induced tumors (Figure 2B). After establishing the presence of NICD in AOM-induced adenomas, the following experiment was undertaken. As described in Materials and methods, AOM-treated

A/J mice were examined for the location and size of adenomas using colonoscopy. After confirming the presence of adenomas in the distal colon (Figure 2C), DAPM (1 mg/kg) or vehicle alone was administered to AOM-treated A/J mice every other day for a total of 4 weeks. Treatment with DAPM did not affect body weight gain throughout the experimental period (data not shown). At sacrifice, no changes were observed in relative liver and spleen weights, nor in colon lengths (data not shown).

At the end of the study, the effects of DAPM treatment on tumorigenesis were determined in methylene blue-stained whole-mount tissues. As shown in Figure 3A, there was a significant reduction in the number of small (<1 mm, $P = 0.04$) and large (>4 mm, $P = 0.03$) tumors in DAPM-treated mice (33 and 60%, respectively). Furthermore, the incidence of large tumors in the DAPM-treated group was markedly lower than that in control group (50 versus 90%, respectively). DAPM treatment also reduced the total number of tumors by ~15% although

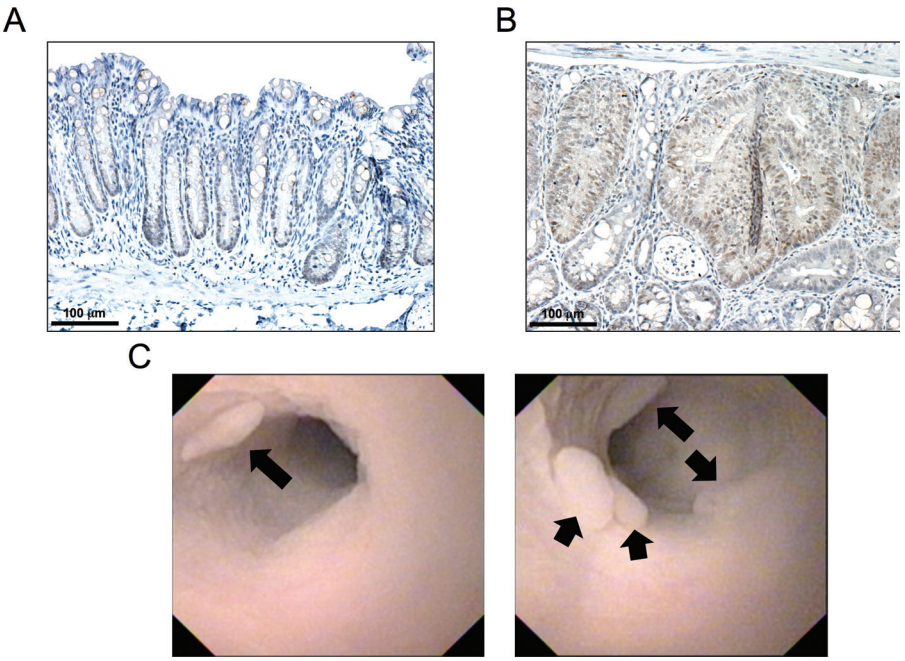

Fig. 2. NICD expression and colonoscopic images of AOM-induced tumors. A/J mice were treated with AOM as described in Materials and methods. Fifteen weeks after the start of treatment, tumors were harvested and prepared for analysis. Representative images for cleaved Notch staining of (**A**) adjacent normal crypts and (**B**) AOM-induced tumors done as described in Materials and methods. (**C**) Representative endoscopic images of AOM-induced tumors. Black arrows indicate the presence of multiple colon tumors within the distal colon at week 15.

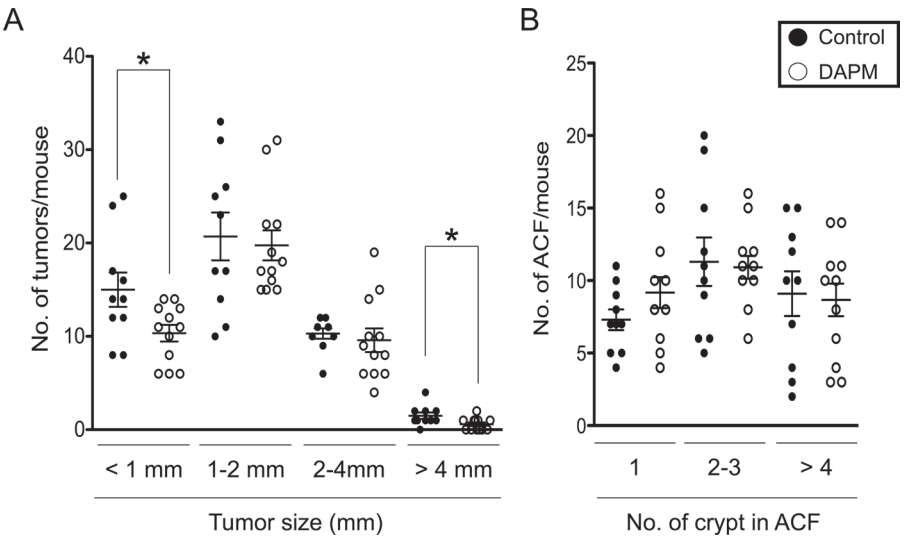

Fig. 3. Effects of DAPM on AOM-induced colon carcinogenesis. A/J mice were treated with AOM as described in Materials and methods. Ten weeks after the last injection of AOM, mice were subjected to colonoscopic examination. After confirmation of tumors, mice were injected i.p. every other day with either DAPM or vehicle (control) for a total of 4 weeks. Mice were killed at week 20 (14 weeks after the last injection of AOM) and the frequency of tumors, and ACF was determined in whole-mount colons using a dissecting microscope. Size distribution of (**A**) tumors and (**B**) ACF in the colons harvested from control ($n = 15$) and DAPM-treated ($n = 15$) mice, respectively. Each data point represent an individual mouse, and the horizontal bars indicate the mean value and standard error for each group. Statistical analysis was performed using the Student's t-test, $^*P < 0.05$ compared with control mice.

the difference was not significant (P = 0.12). Meanwhile, DAPM treatment did not reduce the number of ACF under these experimental conditions (Figure 3B).

Previous studies reported that treatment with a related GSI, dibenzazepine, leads to intestinal goblet cell metaplasia in mice (17,25). To investigate the possibility that DAPM treatment may produce a similar effect in the colon, we examined normal-appearing colonic crypts obtained from vehicle- or DAPM-treated mice using Alcian blue staining to identify goblet cells. As shown in Supplementary Figure S3, available at *Carcinogenesis* Online, mucous granules were larger in DAPM-treated mice compared with the vehicle-treated control group. The number of goblet cells per crypt showed a modest but significant (1.1-fold, $P < 0.01$) increase in the DAPM treatment group.

GSI treatment suppresses cell proliferation and induces tumor-associated KLF4 expression

To determine whether DAPM treatment affects tumor cell proliferation, we evaluated Ki-67 staining (Figure 4A). As shown in Figure 4B, proliferation assessed by the Ki-67 labeling index was significantly decreased in the tumors of GSI-treated mice compared with the control group (41 versus 27%, respectively; $P < 0.001$); importantly, the effect was observed in size-matched tumors as well. KLF4 has been used as a marker for differentiated epithelial cells within the intestine (6). In addition, it is well known that nuclear β-catenin is accumulated within colon tumor cells, but is largely maintained at the cell membrane in differentiated colonocytes (26). Thus, to evaluate the effects of DAPM on differentiation and proliferation of tumor cells, the expression levels of KLF4 and cellular localization of β-catenin were determined in tumor sections by immunofluorescence. As shown in Figure 5A, high levels of KLF4 expression were localized to the upper region of the normal colonic crypt, and β-catenin staining was restricted almost entirely to the lateral cell membranes throughout the normal colonic mucosa adjacent to the tumors. In AOM-induced tumors, however, β-catenin levels were strongly increased within the cytosol, whereas KLF4 expression was markedly decreased (Figure 5B). Importantly, the presence of β-catenin within tumors from DAPM-treated mice tended to localize to the lateral cell membranes, a change that was associated with increased KLF4 immunostaining. In addition, p21 immunostaining was also strongly increased in tumors from the DAPM-treated mice (Figure 5B).

KLF4 is variably expressed in human colon polyps

After establishing the loss of KLF4 expression in carcinogen-induced A/J adenomas, our next goal was to determine the status of KLF4 expression in human polyps. The two most common types of polyps found within the human colon are hyperplastic polyps and non-serrated adenomas (27). Hyperplastic polyps are most common precursor lesion of the serrated neoplasia pathway in the colon and are generally considered to represent a class of colon lesions with less malignant potential (28,29). Tubular adenomas, the most common type of adenoma, have a risk of progression to carcinomas. Confirming previous reports (6,30), KLF4 expression was confined to the middle to upper region of the normal crypt epithelium (Figure 6A). Also shown in Figure 6B, KLF4 expression was readily detected within hyperplastic polyps although the staining was absent from the base of the crypts. However, KLF4 expression was generally absent or dramatically reduced throughout the tubular adenomas, even on the luminal side of the crypts (Figure 6B). Interestingly, β-catenin staining was retained at the cell membrane in the KLF4-expressing hyperplastic cells, but a marked increase in the cytoplasmic localization of β-catenin was associated with a loss of KLF4 expression within the tubular adenomas. Furthermore, most cells that express KLF4 exhibited positive staining for p21 within the hyperplastic polyps (Figure 6C). Meanwhile, the expression levels of p21 were reduced dramatically throughout the tubular adenomas (Figure 6C).

Discussion

There is accumulating evidence that inappropriate activation of Notch signaling plays a key role in cancer pathogenesis (31). Recent efforts have thus been made to suppress this pathway with

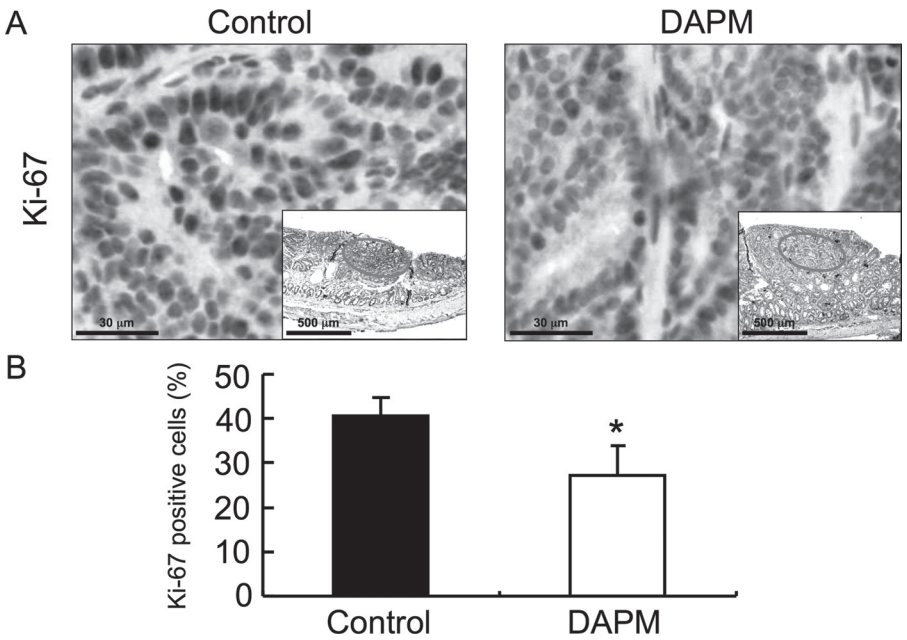

Fig. 4. Ki-67 immunostaining of tumors from control and DAPM-treated mice. Thirty mice were injected with AOM as described in Materials and methods. Ten weeks after the last injection, mice were subjected to colonoscopic imaging to verify the presence of colon tumors. Mice were then administered vehicle (control) or DAPM and killed 4 weeks later. Tissue sections were prepared from the colon of control (n = 15) and DAPM-treated mice (n = 15) and processed for immunohistochemical analysis of Ki-67 as described in Materials and methods. (**A**) Representative images for Ki-67 staining of the tumors from control and DAPM-treated mice (The inset depicts a lower magnification of the tissue and the circled area is shown at the high magnification.) (**B**) The relative percentage of Ki-67-positive cells in the tumor of control and DAPM-treated mice. The positive cells were counted as described in Materials and methods. Columns, mean percent positive cells of 15 samples per group; bars, standard deviation. *$P < 0.05$ compared with control mice (Student's t-test).

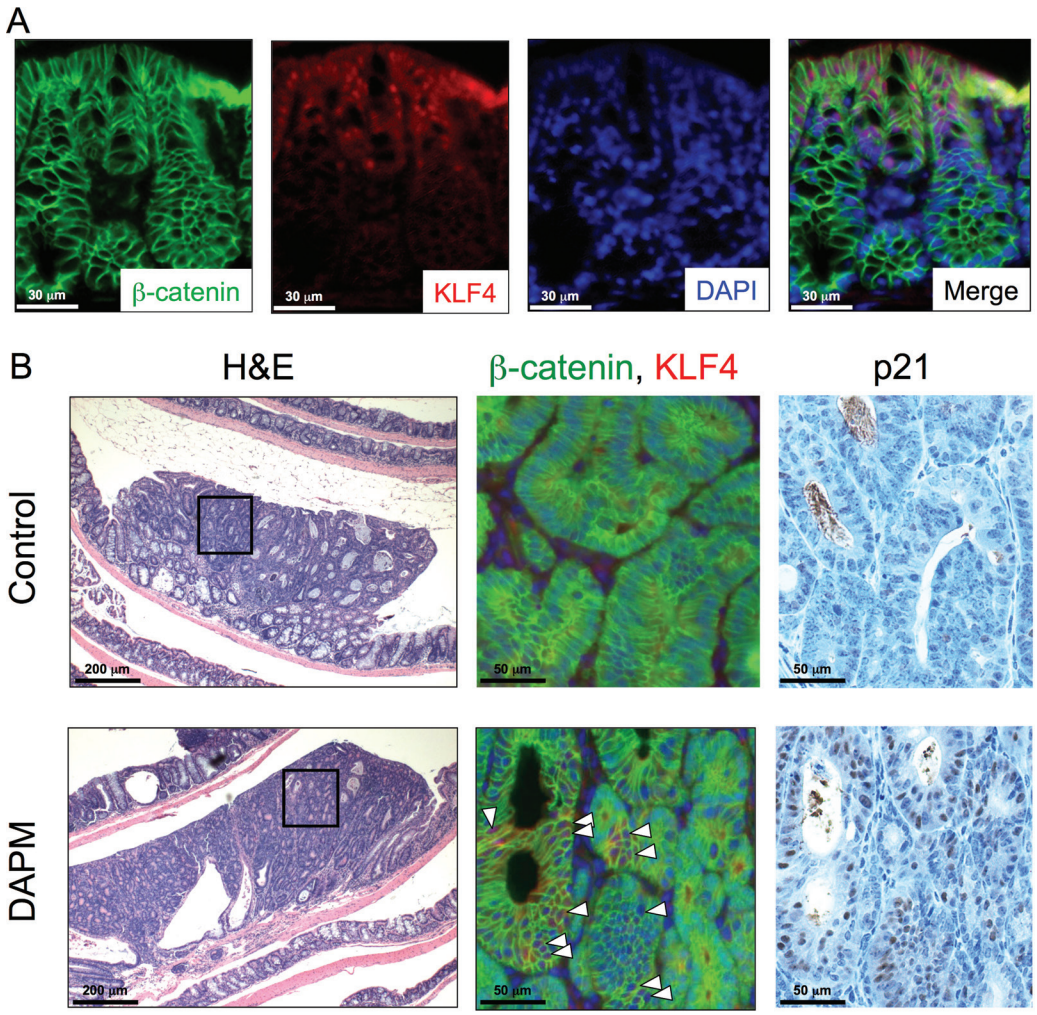

Fig. 5. β-Catenin, KLF4 and p21 expression in AOM-induced colon tumors. DAPM was administered to A/J mice following AOM treatment as described in Materials and methods. Tissue sections were prepared from the colon of control (n = 15) and DAPM-treated mice (n = 15) and processed for immunofluorescent and immunohistochemical analyses as described in Materials and methods. (**A**) Double immunofluorescence staining for β-catenin (green) and KLF4 (red) is shown in normal epithelium adjacent to a colon tumor from untreated control mouse. Nuclei were counterstained with DAPI (blue). Merged images represent the overlay of the β-catenin, KLF4 and DAPI staining. (**B**) Hematoxylin and eosin, β-catenin, KLF4 and p21 staining are shown for tumors from control and DAPM-treated mice. The boxed areas in hematoxylin and eosin sections are enlarged to show areas of positive staining for β-catenin, KLF4 and p21. White arrowheads indicate the KLF4-positive cells within the tumor epithelium. Each serial section was subjected to immunohistochemical analysis of p21.

an expanding repertoire of pharmacologic agents, primarily via inhibition of Notch cleavage (32). Several reports have shown that GSI treatment suppresses intestinal tumor formation in $Apc^{Min/+}$ mice, possibly as a result of the induction of KLF4 (5,17). In light of these promising results, we evaluated the impact of Notch signaling and potential efficacy of a GSI agent employing a colon carcinogenesis model. *N*-[*N*-3,5-difluorophenacetyl]-L-alanyl-*S*-phenylglycine *t*-butyl ester (DAPT) is one of the most commonly used GSI molecules. With respect to DAPM, the ester functional group is attached to a methyl group instead of a *t*-butyl group as found in DAPT. In recent reports, DAPT showed significant efficacy in a mouse wound healing model and also in a fibrosis model at 0.4 and 1.5 mg/kg body weight, respectively (33,34). Based on these studies and the solubility of DAPM, we decided on a dose level of 1 mg/kg body weight for our mouse study. Interestingly, DAPM showed a more potent inhibitory effect for production of Aβ peptides, generated by γ-secretase-mediated cleavage of the amyloid precursor protein, *in vitro* compare with DAPT(35). Indeed, DAPM showed more potent suppressive effect on proliferation of colon cancer cell in our experiment (data not shown). To our knowledge, although, there have been no studies to directly compare the actions of DAPM and DAPT *in vivo*.

In this study, DAPM was found to suppress human cancer cell proliferation via induction of KLF4 and p21 expression *in vitro*. Conversely, $p21^{-/-}$ cells exhibited relative resistance to the suppressive effects of DAPM on cell proliferation compared with the HCT116 WT cells. Furthermore, DAPM treatment effectively suppressed tumor multiplicity and size in AOM-treated A/J mice. The tumor suppression mediated by DAPM treatment is associated with a significant reduction in cell proliferation and increased expression of KLF4 and p21.

Notch signaling is active primarily within the proliferative crypt compartment of the colonic epithelium (36), in contrast to KLF4, which is highly expressed in terminally differentiated epithelial cells (6,37). In a recent animal study, *Klf-4* knockout mice exhibited a reduced number of secretory goblet cells in the colon (38), indicating that KLF4 plays an important role in epithelial homeostasis. Importantly, Notch signaling negatively regulates KLF4 expression through its activation of Hes-1 expression, which is the transcriptional repressor of KLF4 (5). Meanwhile, transgenic expression of NICD increases the number of adenomas in $Apc^{Min/+}$ mice (12) and the level of Notch 1 expression is strongly associated with the pathologic grade of the tumor, as well as its metastatic properties in human colon cancer tissues (39). Conversely, expression of KLF4 is reduced in

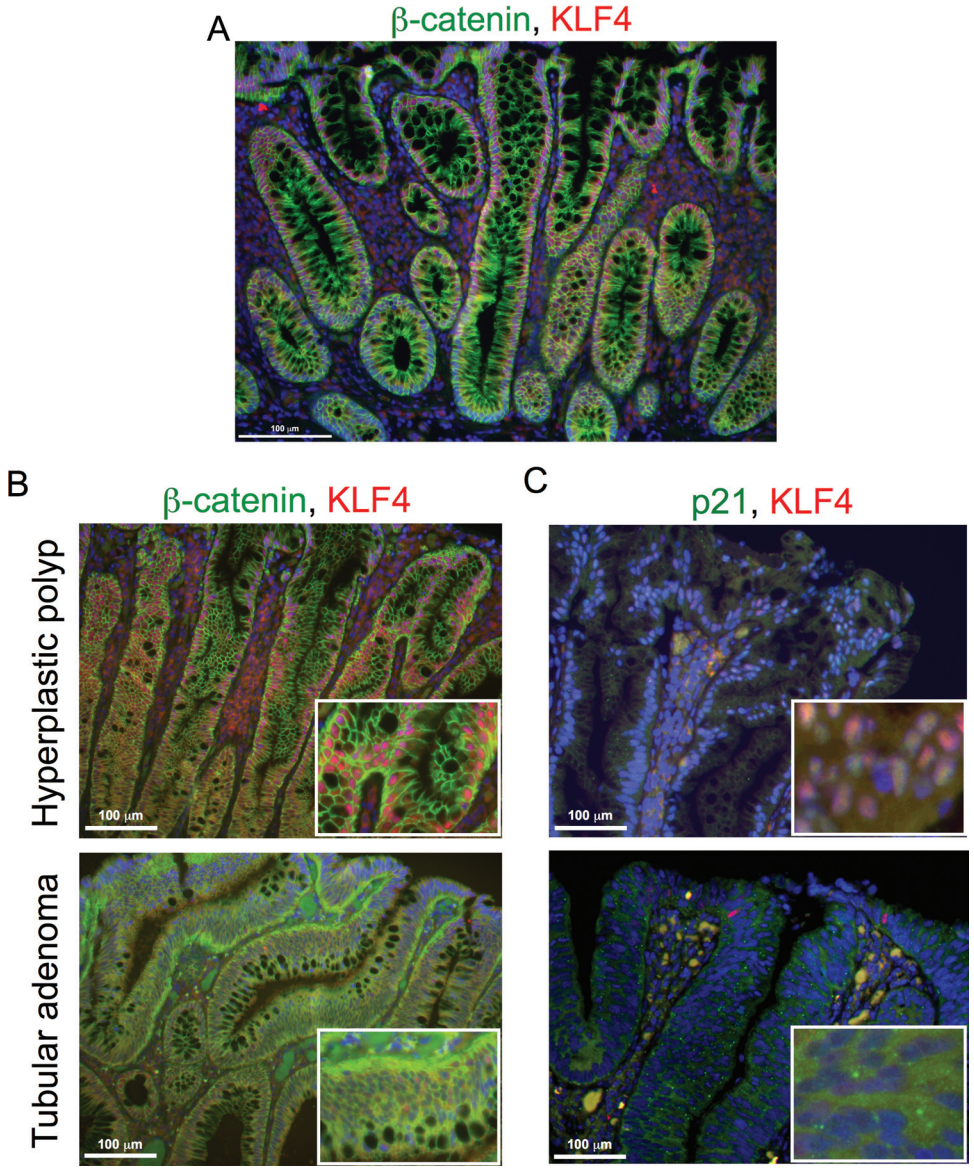

Fig. 6. KLF4, p21 and β-catenin expression in human colon polyps. A panel of 25 human colon polyps was subjected to immunofluorescence staining as described in Materials and methods. Representative expressions of KLF4 (red) and β-catenin (green) immunofluorescence staining of (**A**) normal colonic epithelium and (**B**) colonic polyps (hyperplastic polyp and tubular adenoma). Nuclei were counterstained with DAPI (blue). Insets at the bottom right corner depict an enlarged area of the tumor indicating the extent of positive staining. (**C**) Representative immunofluorescence staining of KLF4 (red) and p21 (green) in a hyperplastic polyp and tubular adenoma. Nuclei were counterstained with DAPI (blue).

colorectal neoplasia, including carcinomas and adenomas, relative to normal mucosa (40). Consistent with these findings, we found higher expression of NICD and lower expression of KLF4 within AOM-induced tumors relative to normal mucosa in mice. Interestingly, in our mouse study, DAPM suppressed tumor numbers, but did not affect the number and size of preneoplastic ACF. Furthermore, as shown in Figure 6, KLF4 was highly expressed in human hyperplastic polyps, a generally benign lesion, but its levels were dramatically reduced or absent within tubular adenomas, a more advanced lesion with a higher risk of progression to adenocarcinoma. Taken together, these observations suggest that inappropriate activation of Notch signaling may occur at early stages of disease progression, especially after the appearance of ACF or formation of hyperplastic lesions.

Synthetic GSIs, which block γ-secretase activity, have shown suppressive effects with respect to cell proliferation in a variety of cancer cell lines, including leukemia, pancreas, lung, breast and colon (5,41–44). Consistent with these earlier studies, as shown in Figure 1, DAPM treatment suppressed cell proliferation and resulted in a concomitant increase in KLF4 and p21 expression in human HCT116 and SW480 colon cancer cells. Previous studies have shown that the ectopic expression of KLF4 in several human colon cancer cell lines results in cell cycle arrest (45–47). Furthermore, the activation (p21) and repression (cyclins B1 and D1) of several key transcriptional targets of KLF4 plays a fundamental role in the control of cellular differentiation and cell cycle inhibition (46). Indeed, we showed that p21-null HCT 116 cells were largely resistant to the suppressive effects of DAPM on cell proliferation compared with the parental control cells. Furthermore, the Ki-67 labeling index was significantly reduced in tumors from the DAPM-treated mice, a response that is associated with elevated KL4 and p21 expression. Taken together, we postulate that DAPM may suppress tumor growth by inducing cell cycle arrest through its upregulation of KLF4 and p21 expression. However, since DAPM moderately suppressed cell proliferation in p21-null cells, it is possible that additional mechanisms may contribute to the tumor-suppressive effects of DAPM. In the past, several Notch target genes have been identified, including nuclear

factor-kappa B, cyclooxygenase-2, vascular endothelial growth factor, matrix metalloproteinase-9, extracellular-regulated kinase, Akt, cyclin D1, c-myc, $p27^{kip1}$ and *p53*, in human cancer cells (31). Most of these proteins are closely associated with proliferation and survival of cancer cells and thus represent potential targets for chemoprevention (48). Taken together, the downregulation of these genes by DAPM might uncover additional mechanisms that contribute to the tumor-suppressive effects of DAPM observed in this study.

Within this context, the potential for cross-talk between β-catenin and KLF4 or possibly Notch, must also be considered. β-Catenin is phosphorylated by a cytoplasmic destruction complex consisting of glycogen synthase kinase 3β (GSK3β), adenomatous polyposis coli (APC) and axin, and it is targeted for proteasomal degradation in the absence of Wnt signaling (49). Activation of Wnt signaling disrupts the β-catenin destruction complex, enabling the levels of unphosphorylated (active) β-catenin protein to accumulate, functioning in turn as a coactivator for the transcription factor T-cell factor/lymphoid enhancer factor (49). It is well known that Wnt/β-catenin signaling plays an essential role in both normal development and tumorigenesis (50). In this study, we found that β-catenin was located primarily at the cell membrane in KLF4-expressing cells within human hyperplastic polyps. Meanwhile, β-catenin staining was found to accumulate within the cytosol of more advanced tubular adenomas, particularly in the absence of KLF4 expression. Furthermore, in our mouse study, β-catenin tended to be localized at the cell membrane within KLF4-expressing tumor cells in DAPM-treated mice. Interestingly, Kwon *et al.* (51,52) showed that uncleaved membrane-bound (full length) Notch directly associates with active β-catenin in its membrane-tethered state and negatively regulates translocation of active β-catenin into the nucleus in colon cancer cells. Meanwhile, Zhang *et al.* (53) showed that KLF4 directly interacts with β-catenin and inhibits its transcriptional activation, resulting in induction of cell cycle arrest. Taken together, these results suggest that maintaining full-length Notch by DAPM treatment suppresses the activation of Wnt signaling by tethering active β-catenin to the plasma membrane and/or inducing KLF4 expression, thereby contributing to the suppression of AOM-induced colon carcinogenesis. This may provide a novel therapeutic mechanism for GSI activity in colon cancer prevention.

In conclusion, we have demonstrated for the first time that treatment of mice with the GSI, DAPM, suppresses the growth of colon adenomas. The protective effects of DAPM are most likely mediated through the KLF4-p21 axis, as well as via effects on β-catenin cellular trafficking. In addition, we have found that KLF4 is highly expressed in human hyperplastic polyps, but its levels are dramatically reduced or even absent within more advanced tubular adenomas. Taken together, our results imply that inhibition of Notch cleavage by pharmacologic intervention may suppress tumor proliferation via the induction of KLF4 and p21 expression, as well as inhibition of Wnt signaling. Based on these findings, GSI may represent a promising approach for the prevention of colon cancer. Furthermore, these results suggest that KLF4 provides a promising surrogate marker that may be used to further distinguish molecular changes between hyperplasia and dysplasia.

Supplementary material

Supplementary Table S1 and Figures S1–S3 can be found at http://carcin.oxfordjournals.org/

Funding

National Institutes of Health (CA125691 to D.W.R.).

Acknowledgements

The authors are indebted to Dr Thiruchandurai V. Rajan for his comprehensive pathological analyses of human specimens. The authors would also like to thank Dr Bert Vogelstein (Jones Hopkins University, Baltimore, MD) for generously providing the wild-type and $p21^{-/-}$ variant of HCT116 cells.

Conflict of Interest Statement: None declared.

References

1. Artavanis-Tsakonas,S. *et al.* (1999) Notch signaling: cell fate control and signal integration in development. *Science*, **284**, 770–776.
2. Baron,M. (2003) An overview of the Notch signalling pathway. *Semin. Cell Dev. Biol.*, **14**, 113–119.
3. Iso,T. *et al.* (2003) HES and HERP families: multiple effectors of the Notch signaling pathway. *J. Cell. Physiol.*, **194**, 237–255.
4. Katoh,M. *et al.* (2007) Notch signaling in gastrointestinal tract (review). *Int. J. Oncol.*, **30**, 247–251.
5. Ghaleb,A.M. *et al.* (2008) Notch inhibits expression of the Krüppel-like factor 4 tumor suppressor in the intestinal epithelium. *Mol. Cancer Res.*, **6**, 1920–1927.
6. Shields,J.M. *et al.* (1996) Identification and characterization of a gene encoding a gut-enriched Krüppel-like factor expressed during growth arrest. *J. Biol. Chem.*, **271**, 20009–20017.
7. Abbas,T. *et al.* (2009) p21 in cancer: intricate networks and multiple activities. *Nat. Rev. Cancer*, **9**, 400–414.
8. Ellisen,L.W. *et al.* (1991) TAN-1, the human homolog of the Drosophila notch gene, is broken by chromosomal translocations in T lymphoblastic neoplasms. *Cell*, **66**, 649–661.
9. Lobry,C. *et al.* (2011) Oncogenic and tumor suppressor functions of Notch in cancer: it's NOTCH what you think. *J. Exp. Med.*, **208**, 1931–1935.
10. Reedijk,M. *et al.* (2008) Activation of Notch signaling in human colon adenocarcinoma. *Int. J. Oncol.*, **33**, 1223–1229.
11. Fre,S. *et al.* (2005) Notch signals control the fate of immature progenitor cells in the intestine. *Nature*, **435**, 964–968.
12. Fre,S. *et al.* (2009) Notch and Wnt signals cooperatively control cell proliferation and tumorigenesis in the intestine. *Proc. Natl Acad. Sci. USA*, **106**, 6309–6314.
13. Moser,A.R. *et al.* (1990) A dominant mutation that predisposes to multiple intestinal neoplasia in the mouse. *Science*, **247**, 322–324.
14. Kadaveru,K. *et al.* (2012) Dietary Methyl Donor Depletion Protects Against Intestinal Tumorigenesis in ApcMin/+ Mice. *Cancer Prevent. Res.*, **5**, 911–920.
15. Rodilla,V. *et al.* (2009) Jagged1 is the pathological link between Wnt and Notch pathways in colorectal cancer. *Proc. Natl Acad. Sci. USA,* **106**, 6315–6320.
16. Wolfe,M.S. *et al.* (1998) A substrate-based difluoro ketone selectively inhibits Alzheimer's gamma-secretase activity. *J. Med. Chem.*, **41**, 6–9.
17. van Es,J.H. *et al.* (2005) Notch/gamma-secretase inhibition turns proliferative cells in intestinal crypts and adenomas into goblet cells. *Nature*, **435**, 959–963.
18. Papanikolaou,A. *et al.* (2000) Sequential and morphological analyses of aberrant crypt foci formation in mice of differing susceptibility to azoxymethane-induced colon carcinogenesis. *Carcinogenesis*, **21**, 1567–1572.
19. Nambiar,P.R. *et al.* (2002) Role of the alternating reading frame (P19)-p53 pathway in an *in vivo* murine colon tumor model. *Cancer Res.*, **62**, 3667–3674.
20. Guda,K. *et al.* (2004) Carcinogen-induced colon tumors in mice are chromosomally stable and are characterized by low-level microsatellite instability. *Oncogene*, **23**, 3813–3821.
21. Rosenberg,D.W. *et al.* (2009) Mouse models for the study of colon carcinogenesis. *Carcinogenesis*, **30**, 183–196.
22. Nakanishi,M. *et al.* (2007) Utilizing endoscopic technology to reveal real-time proteomic alterations in response to chemoprevention. *Proteomics. Clin. Appl.*, **1**, 1660–1666.
23. Becker,C. *et al.* (2006) High resolution colonoscopy in live mice. *Nat. Protoc.*, **1**, 2900–2904.
24. Nakanishi,M. *et al.* (2011) Selective PGE(2) suppression inhibits colon carcinogenesis and modifies local mucosal immunity. *Cancer Prev. Res.*, **4**, 1198–1208.
25. Murata,K. *et al.* (2005) Hes1 directly controls cell proliferation through the transcriptional repression of p27Kip1. *Mol. Cell. Biol.*, **25**, 4262–4271.
26. van de Wetering,M. *et al.* (2002) The beta-catenin/TCF-4 complex imposes a crypt progenitor phenotype on colorectal cancer cells. *Cell*, **111**, 241–250.
27. Carr,N.J. *et al.* (2009) Serrated and non-serrated polyps of the colorectum: their prevalence in an unselected case series and correlation of BRAF mutation analysis with the diagnosis of sessile serrated adenoma. *J. Clin. Pathol.*, **62**, 516–518.
28. Torlakovic,E. *et al.* (2003) Morphologic reappraisal of serrated colorectal polyps. *Am. J. Surg. Pathol.*, **27**, 65–81.

29. Higuchi,T. *et al.* (2005) Demographic and pathological characteristics of serrated polyps of colorectum. *Histopathology*, **47**, 32–40.
30. Garrett-Sinha,L.A. *et al.* (1996) A gene for a novel zinc-finger protein expressed in differentiated epithelial cells and transiently in certain mesenchymal cells. *J. Biol. Chem.*, **271**, 31384–31390.
31. Ranganathan,P. *et al.* (2011) Notch signalling in solid tumours: a little bit of everything but not all the time. *Nat. Rev. Cancer*, **11**, 338–351.
32. Shih,I.e.M. *et al.* (2007) Notch signaling, gamma-secretase inhibitors, and cancer therapy. *Cancer Res.*, **67**, 1879–1882.
33. Dees,C. *et al.* (2011) Inhibition of Notch signaling prevents experimental fibrosis and induces regression of established fibrosis. *Arthritis Rheum.*, **63**, 1396–1404.
34. higurupati,S. *et al.* (2007) Involvement of notch signaling in wound healing. *PLoS One*, **2**, e1167.
35. Czvitkovich,S. *et al.* (2011) Comparison of pharmacological modulation of APP metabolism in primary chicken telencephalic neurons and in a human neuroglioma cell line. *J. Mol. Neurosci.*, **43**, 257–267.
36. Miyamoto,S. *et al.* (2011) Role of Notch signaling in colon homeostasis and carcinogenesis. *Cancer Sci.*, **102**, 1938–1942.
37. Dang,D.T. *et al.* (2000) The biology of the mammalian Krüppel-like family of transcription factors. *Int. J. Biochem. Cell Biol.*, **32**, 1103–1121.
38. Katz,J.P. *et al.* (2002) The zinc-finger transcription factor Klf4 is required for terminal differentiation of goblet cells in the colon. *Development*, **129**, 2619–2628.
39. Zhang,Y. *et al.* (2010) Notch1 regulates the growth of human colon cancers. *Cancer*, **116**, 5207–5218.
40. Xu,J. *et al.* (2008) Dynamic down-regulation of Krüppel-like factor 4 in colorectal adenoma-carcinoma sequence. *J. Cancer Res. Clin. Oncol.*, **134**, 891–898.
41. Real,P.J. *et al.* (2009) Gamma-secretase inhibitors reverse glucocorticoid resistance in T cell acute lymphoblastic leukemia. *Nat. Med.*, **15**, 50–58.
42. Plentz,R. *et al.* (2009) Inhibition of gamma-secretase activity inhibits tumor progression in a mouse model of pancreatic ductal adenocarcinoma. *Gastroenterology*, **136**, 1741–9.e6.
43. Maraver,A. *et al.* (2012) Therapeutic effect of γ-secretase inhibition in KrasG12V-driven non-small cell lung carcinoma by derepression of DUSP1 and inhibition of ERK. *Cancer Cell*, **22**, 222–234.
44. Rasul,S. *et al.* (2009) Inhibition of gamma-secretase induces G2/M arrest and triggers apoptosis in breast cancer cells. *Br. J. Cancer*, **100**, 1879–1888.
45. Chen,X. *et al.* (2001) Krüppel-like factor 4 (gut-enriched Krüppel-like factor) inhibits cell proliferation by blocking G1/S progression of the cell cycle. *J. Biol. Chem.*, **276**, 30423–30428.
46. Yoon,H.S. *et al.* (2003) Kruppel-like factor 4 mediates p53-dependent G1/S cell cycle arrest in response to DNA damage. *J. Biol. Chem.*, **278**, 2101–2105.
47. Yoon,H.S. *et al.* (2004) Requirement of Krüppel-like factor 4 in preventing entry into mitosis following DNA damage. *J. Biol. Chem.*, **279**, 5035–5041.
48. Surh,Y.J. (2003) Cancer chemoprevention with dietary phytochemicals. *Nat. Rev. Cancer*, **3**, 768–780.
49. Logan,C.Y. *et al.* (2004) The Wnt signaling pathway in development and disease. *Annu. Rev. Cell Dev. Biol.*, **20**, 781–810.
50. Reya,T. *et al.* (2005) Wnt signalling in stem cells and cancer. *Nature*, **434**, 843–850.
51. Kwon,C. *et al.* (2009) A regulatory pathway involving Notch1/beta-catenin/Isl1 determines cardiac progenitor cell fate. *Nat. Cell Biol.*, **11**, 951–957.
52. Kwon,C. *et al.* (2011) Notch post-translationally regulates β-catenin protein in stem and progenitor cells. *Nat. Cell Biol.*, **13**, 1244–1251.
53. Zhang,W. *et al.* (2006) Novel cross talk of Kruppel-like factor 4 and beta-catenin regulates normal intestinal homeostasis and tumor repression. *Mol. Cell. Biol.*, **26**, 2055–2064.

Received January 15, 2013; revised May 22, 2013; accepted May 27, 2013